Microelectronics Reliability 62 (2016) 124–129

Contents lists available at ScienceDirect

Microelectronics Reliability

journal homepage: www.elsevier.com/locate/mr

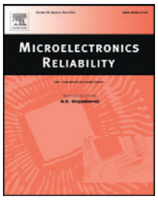

Climate specific thermomechanical fatigue of flat plate photovoltaic module solder joints

Nick Bosco *, Timothy J. Silverman, Sarah Kurtz

National Renewable Energy Laboratory, 15013 Denver West Parkway Golden, CO 80401-3305, USA

ARTICLE INFO

Article history:
Received 21 September 2015
Received in revised form 14 March 2016
Accepted 14 March 2016
Available online 24 March 2016

Keywords:
Photovoltaic reliability
Solder fatigue
Acceleration factor
Thermal cycling

ABSTRACT

FEM simulations of PbSn solder fatigue damage are used to evaluate seven cities that represent a variety of climatic zones. It is shown that the rate of solder fatigue damage is not ranked with the cities' climate designations. For an accurate ranking, the mean maximum daily temperature, daily temperature change and a characteristic of clouding events are all required. A physics-based empirical equation is presented that accurately calculates solder fatigue damage according to these three factors. An FEM comparison of solder damage accumulated through service and thermal cycling demonstrates the number of cycles required for an equivalent exposure. For an equivalent 25-year exposure, the number of thermal cycles (−40 °C to 85 °C) required ranged from roughly 100 to 630 for the cities examined. It is demonstrated that increasing the maximum cycle temperature may significantly reduce the number of thermal cycles required for an equivalent exposure.

Published by Elsevier Ltd.

1. Introduction

Solder joints that attach stringing ribbons to cells within a PV module will experience thermomechanical fatigue with outdoor exposure. Increasing thermomechanical fatigue will cause these joints to first crack and then ultimately fail. This PV module degradation mechanism will manifest as a loss of power due to a series resistance increase and, in the extreme case, total power loss due to an open circuit [1]. The rate of thermomechanical fatigue within these joints depends on several factors such as module design, materials selection and exposure conditions [2].

The purpose of this paper is to examine the specific weather characteristics that drive solder fatigue damage and to quantify how much this damage may vary with climate zone and specific deployment location. This work is motivated by a recent survey of PV module degradation made across India [3]. In this survey, modules that showed visible degradation upon inspection were further examined for their electrical characteristics. The survey showed that modules deployed in the hot climates exhibited power degradation due to an increase in series resistance, while the modules deployed in the cooler climates had a lower degradation in power that was not significantly influenced by a series resistance increase. A similar observation of modules deployed in hot climates exhibiting larger power degradation due to an increase in series resistance was also reported by Jordan et al. who examined more than 2000 PV degradation rates quoted in publications for locations around the world [4]. Because failing solder joints will result in an increase in series resistance, they proposed this as a possible mechanism for the higher degradation rates of the modules deployed in hotter climates.

We begin this work by developing a finite element model (FEM) of a flat plate module to calculate the accumulation of inelastic strain energy density (damage) within the solder joint through exposure to a temperature history. Simulations are then run to calculate the accumulation of solder damage both when the module is deployed in specific cities across a range of climatic zones and through accelerated thermal cycling. Simulations of one year in seven cities are conducted, and the solder damage accumulated is directly compared to a variety of accelerated thermal cycles. Finally, an empirical equation is presented that calculates solder damage for the modeled module based on simple, specific weather characteristics.

2. Methods

2.1. Cities

We chose seven cities to evaluate in this study. They include Chennai and Bhogat in India and Golden Colorado, Phoenix and Tucson Arizona, Sioux Falls South Dakota and Honolulu Hawaii all in the United States. These cities were chosen because they represent a variety of climate zones and possess weather-monitoring sites that collect high-resolution meteorological data available for our analysis. Table 1 presents these cities and their climatic zones according to the criteria followed in the All-India Survey, Table 2. These criteria define five climatic zones by their mean monthly maximum temperature and mean relative humidity. The five climatic zones include Hot and Dry,

---

* Corresponding author.

http://dx.doi.org/10.1016/j.microrel.2016.03.024
0026-2714/Published by Elsevier Ltd.

Table 1
The seven cities examined in this study and their climatic zone as designated by their mean monthly maximum temperature.

City	Climate	Mean monthly max temp (C)
Phoenix	Hot and Dry	38
Chennai	Hot and Humid	37
Tucson	Hot and Dry	36
Bhogat	Hot and Humid	35
Honolulu	Hot and Humid	31
Golden	Temperate	27
Sioux Falls	Cold	23

Hot and Humid, Temperate, Cold and Composite. Because solder fatigue is not directly influenced by humidity, only temperature was considered for this study.

2.2. FEM model

A 2D cross-sectional model of a generic crystalline silicon flat plate module was generated using COMSOL. The 2D simplification was made to produce a model capable of simulating years of weather exposure within a reasonable computational time. Because of the large aspect ratio of the PV module, the plane strain condition imposed by the 2D simplification is a reasonable approximation and yields a model that accurately captures the physics of solder behavior within the module. The module laminate was modeled to have 12 cells along its length and a glass/polymer backsheet construction as detailed in Fig. 1 and Table 3. The glass front sheet is 3.6 mm thick, the silicon cells 175 μm thick with 150 μm copper ribbons attached with 30 μm of PbSn eutectic solder and encapsulated in 450 μm of EVA. The backsheet was modeled as a single 175 μm layer with elastic properties representing the appropriate contribution of its laminate's components. This simplification was made to increase the minimum model element thickness. The rate-dependent creep behavior and the time-independent plasticity of the solder were characterized by the Anand's model [5]. All other materials were modeled as linear-elastic, with properties as detailed in Table 3.

Darveaux's approach was taken to evaluate the solder's damage accumulation. Derived from the Paris power law of fatigue crack growth, the Darveaux approach considers the accumulation of inelastic strain energy density as a damage indicator for fatigue crack growth [6]. Accordingly, both crack initiation and crack growth are functions of the average inelastic strain energy density (plastic work) accumulated per loading cycle. In the current study, the two phases of failure were not differentiated, therefore only the total plastic work was considered as the metric for damage.

A model refinement was conducted to provide a level of confidence in our simulations. The 85 °C thermal cycle, as described in the following section, was used for this purpose and simulations run for models of decreasing mesh size (coarse 3, to fine 0.5), or increasing degrees of freedom. The goal was to create a model that would provide accurate results within a reasonable computational time. For each model, eleven thermal cycles were simulated. By the 10th cycle, the finest model was within 0.8% of its 11th cycle's damage value. We found that the damage accumulated by each model decreased with each successive cycle and all models settled within 5% of the finest model's final cycle value by the tenth cycle, Fig. 2. While the coarsest model we considered rendered an 11th cycle damage value within 5% of our finest model, we settled on the second coarsest model for the remainder of our study, Fig. 3. Furthermore, it was found that the solder joints on the bottom (backsheet side) of the cells accumulate damage at a rate more than 4 times faster than on the top of the cells, therefore; only the damage accumulated at the bottom of the middle cell was modeled and reported for the subsequent simulations.

Table 2
Climatic zone designations as defined by the All-India Survey.

Climate	Mean monthly max temp (C)	Mean relative humidity (%)
Hot and Dry	>30	<55
Hot and Humid	>30	>55
	>25	>75
Temperate	25–30	<75
Cold	<25	All values
Composite	When 6 months or more do not fall within any of the above categories	

2.3. Simulations

2.3.1. Thermal cycling

Two types of simulations were conducted in this study: weather and thermal cycles. The thermal cycles represent interpretations of the thermal cycles designated in IEC 61215 — Crystalline Silicon Terrestrial PV modules — design qualification and type approval. All cycles have temperature ramp rates of 2 °C/min, a minimum temperature of −40 °C and 10-min cold and hot dwell times. The four cycles simulated are, therefore, designated by their hot dwell temperatures: 85, 90, 95 and 100 °C. The damage reported for these cycles is the damage accumulated during the tenth successive cycle simulated.

2.3.2. Weather

A one-year history of module cell temperature was synthesized by examining meteorological data in each of the seven cities examined in this study. Ambient temperature, T_{amb}, wind speed, WS, and total global irradiance, E, collected at one-minute intervals served as input into a steady state temperature model developed by King et al. to calculate cell temperature [7]:

$$T_{cell} = T_{amb} + E \cdot \exp(a + b \cdot WS) + E\frac{\Delta T}{E_o}. \tag{1}$$

The coefficients a and b were empirically determined for a glass/polymer backsheet module construction deployed in an open-rack configuration to be −3.56 and −0.075, respectively [7]. E_o is the reference solar irradiance of 1000 W/m^2 and ΔT represents the temperature difference between the cell and module at this reference irradiance. For an open-rack configuration ΔT was determined to be 3 °C; however, this offset temperature will be sensitive to racking method and module construction.

To capture transient behavior, an exponentially weighted moving-average (EWMA) filter with a time constant derived from experimental module temperature data was applied to the static model. Cell temperature at time step t is calculated using:

$$(T_{cell})_t = (T_{cell})_{t-1}\alpha + (T_{cell})_t(1-\alpha) \tag{2}$$

where α is the EWMA gain, 0.8. This method of synthesizing module cell temperature from meteorological data allows a more level comparison of location by removing the variability of specific module temperature measurements.

Simulations using this synthesized module cell temperature were run in one-month intervals. To account for the model's tendency to require a length of simulated time before settling to a constant damage rate, the first six days of each month were added to the end of the simulation. The damage calculated for each month, therefore, only considered the first six days the second time they were simulated.

3. Results and analysis

3.1. Thermal cycling

An image illustrating the accumulation of inelastic strain energy within the modeled module's solder joints is presented in Fig. 4. The